doi:10.1246/cl.2010.864
Published on the web July 10, 2010

Structure and Photovoltaic Properties of (*E*)-2-Cyano-3-[4-(diphenylamino)phenyl]acrylic Acid Substituted by *tert*-Butyl Groups

Katsuhiko Ono,*[1] Tomoya Yamaguchi,[1] and Masaaki Tomura[2]
[1]*Department of Materials Science and Engineering, Nagoya Institute of Technology, Gokiso, Showa-ku, Nagoya, Aichi 466-8555*
[2]*Institute for Molecular Science, Myodaiji, Okazaki, Aichi 444-8585*

(Received May 10, 2010; CL-100455; E-mail: ono.katsuhiko@nitech.ac.jp)

(*E*)-3-{4-[Bis(4-*tert*-butylphenyl)amino]phenyl}-2-cyanoacrylic acid and its related compounds were synthesized by the Knoevenagel condensation of the corresponding 4-aminobenzaldehydes with cyanoacetic acid. Cyclic voltammetry measurements showed that these organic dyes exhibited reversible oxidation waves. The *tert*-butyl substituents also decreased molecular stacking in the crystals, thus affecting the photovoltaic properties of the dyes. A solar cell using the *tert*-butyl-substituted dye exhibited higher performance than that for the analog without *tert*-butyl group substitution.

The fabrication of low cost and high performance dye-sensitized solar cells (DSCs) has attracted considerable attention.[1] DSCs using ruthenium sensitizers exhibited a solar energy-to-electricity conversion efficiency (η) above 11% at standard AM 1.5 solar light.[2] Recently, DSCs using metal-free organic dyes have been intensely studied. A number of organic dyes, such as triphenylamine,[3–5] carbazole,[6,7] coumarin,[8] indoline,[9] heteroanthracene,[10] and phthalocyanine dyes[11] have been synthesized and investigated. DSCs incorporating these dyes exhibit conversion efficiencies ranging within 4–10%. The major factors decreasing conversion efficiencies are the formation of dye aggregates on the TiO_2 electrodes and the recombination of excited electrons.[4a,6b] In this regard, we introduced *tert*-butyl groups into (*E*)-2-cyano-3-[4-(diphenylamino)phenyl]acrylic acid (CDPA)[12] to generate dye **1** and its analogs **2** and **3** (Scheme 1). These dyes have simple donor–π–acceptor structures, which are easily modified into extended π-conjugation systems.[3,7,13] Therefore, significant information is obtained about the *tert*-butyl substituent effects. In this paper, we report the synthesis, properties, and crystal structures of organic dyes **1**–**3** and their application to DSCs.

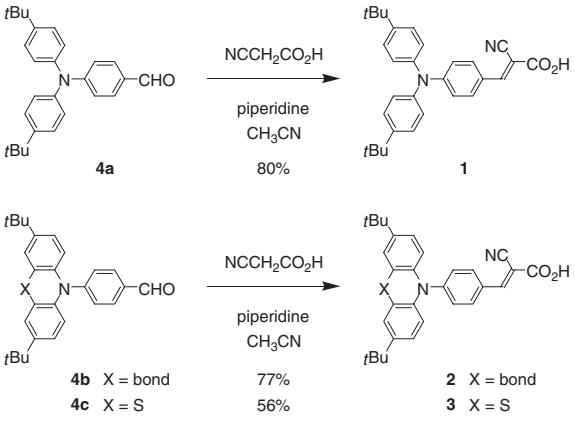

Scheme 1. Synthesis of organic dyes **1**–**3**.

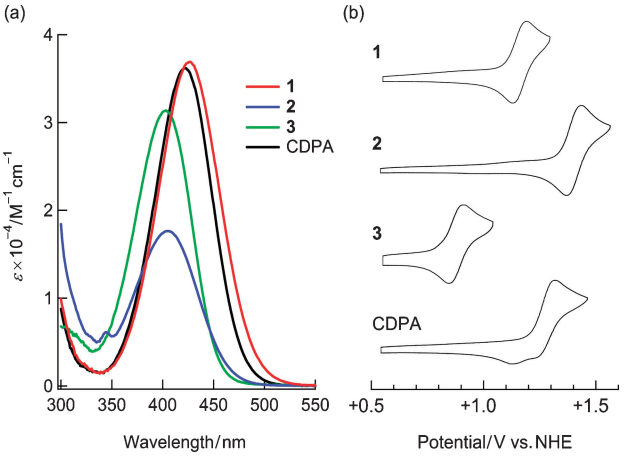

Figure 1. (a) UV–vis absorption spectra and (b) cyclic voltammograms of **1**–**3** in acetonitrile.

Table 1. UV–vis absorption properties and oxidation potentials of dyes **1**–**3** in acetonitrile

Dye	λ_{max}/nm (ε)	E_{gap}/eV	$E_{1/2}^{ox}$/V[a]
1	426 (36900)	2.54	+1.17
2	406 (17600)	2.67	+1.40
3	403 (31400)	2.73	+0.88
CDPA	422 (36200)	2.60	+1.29[b]

[a]V versus NHE, ref. 15. [b]Irreversible: $E_p^{ox} - 0.03$ V.

The synthesis of organic dyes **1**–**3** is illustrated in Scheme 1.[14] The dyes were prepared in 56–80% yields by the Knoevenagel condensation of 4-aminobenzaldehydes **4a**–**4c** with cyanoacetic acid in the presence of piperidine. Structural determinations of the dyes were performed using spectroscopic and elemental analyses. The dyes were obtained as orange crystals or a yellow solid, and their melting points were above 200 °C. UV–vis absorption spectra of **1**–**3** in acetonitrile are shown in Figure 1a. The absorption maximum of **1** was slightly red-shifted compared to that of CDPA, and the HOMO–LUMO energy gap (E_{gap}) of **1** was smaller than for CDPA (Table 1). This indicates that *tert*-butyl groups slightly enhance the donor–π–acceptor character of the CDPA skeleton. On the other hand, the absorption maxima of **2** and **3** were blue-shifted compared to that of **1**, and the HOMO–LUMO energy gaps of **2** and **3** were larger than that of **1**. Therefore, bis(4-*tert*-butylphenyl)amine groups facilitate absorption at long wavelengths.

Cyclic voltammetry (CV) measurements in acetonitrile were performed to investigate the redox properties of **1**–**3**.[15] The

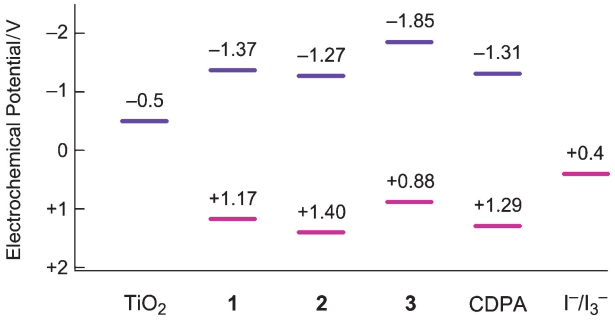

Figure 2. Electrochemical potential diagram of dyes **1**–**3** in volts versus NHE: the oxidation potentials of ground states (—) and excited states (—).

voltammograms displayed reversible oxidation waves for **1**–**3** (Figure 1b). CDPA showed an irreversible oxidation wave at +1.32 V versus normal hydrogen electrode (NHE), suggesting that the *tert*-butyl groups stabilize the cation radical species generated by CV scanning. The oxidation potential of **1** was slightly negative compared to that of CDPA. On the other hand, oxidation potentials varied depending on the nature of the amines. The potential of **1** was more negative than that for **2**, but was in the positive when compared to **3** (Table 1).

Figure 2 shows the electrochemical potential diagrams of dyes **1**–**3** in volts versus NHE. The oxidation potentials of the excited dyes were calculated from the difference between their halfwave oxidation potential ($E_{1/2}^{ox}$) and their HOMO–LUMO energy gap (E_{gap}), $E_{1/2}^{ox} - E_{gap}$.[4a] The oxidation potentials of excited dyes **1**–**3** are sufficiently more negative than the potential of the TiO_2 conduction band (−0.5 V),[1b] suggesting an effective electron injection from the excited dyes to the TiO_2 electrodes in DSCs. The oxidation potentials of **1**–**3** in the ground states are more positive than the I^-/I_3^- redox potential (+0.4 V), suggesting the effective reduction of the oxidized dyes by iodine.

The molecular structures of **1** and CDPA[16] were investigated by X-ray crystallography.[14,17] Single crystals of **1** and CDPA were grown by recrystallization from their acetonitrile solutions. Compound **1** gave two crystal forms; one with and one without acetonitrile,[18] and the structure of the crystal obtained without acetonitrile has been successfully elucidated. Two crystallographically independent molecules were observed in the crystal. Bond distances and angles were almost identical for **1** and CDPA (Figures 3a–3c).[14] The (*E*)-2-cyano-3-phenylacrylic acid moieties were found to be planar and to form hydrogen-bonded carboxylic acid dimers. The dimer units stacked into columnar structures which featured intermolecular distances of 3.42 Å for CDPA (Figure 3d) and 3.61 Å for **1** (Figure 3e). The stacking distance between CDPA molecules was similar to the sum of the van der Waals radii for carbon atoms (C···C = 3.40 Å), suggesting the presence of intermolecular interactions in the column. On the other hand, the stacking distance was much larger than the sum of the van der Waals carbon atom radii for **1**, indicating that the *tert*-butyl groups sterically hinder molecular stacking in the crystal. In addition, the second molecular structure of **1** was not columnar (Figure 3f). Therefore, the introduction of *tert*-butyl groups in a CDPA backbone may prove significantly effective in inhibiting molecular aggregation on TiO_2 electrodes.

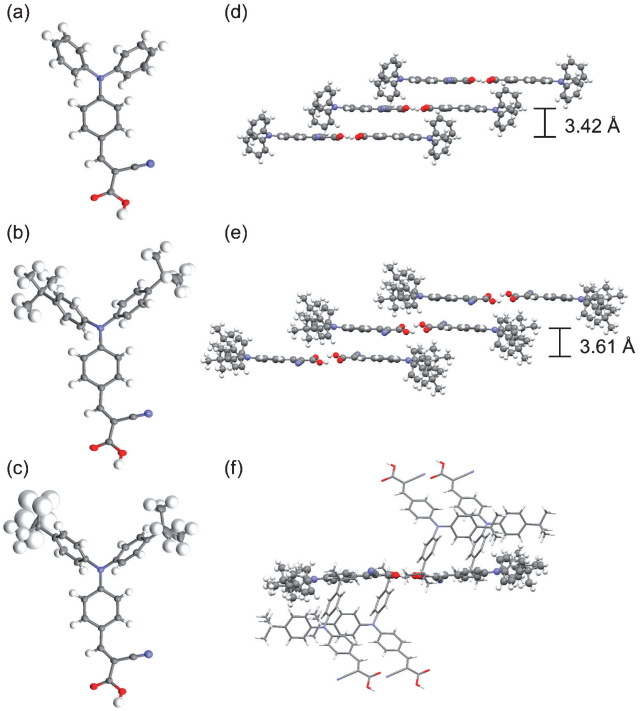

Figure 3. X-ray crystallography: molecular structures (ellipsoid) of CDPA (a) and **1** (b, c) and packing modes (ball and stick) of CDPA (d) and **1** (e, f).

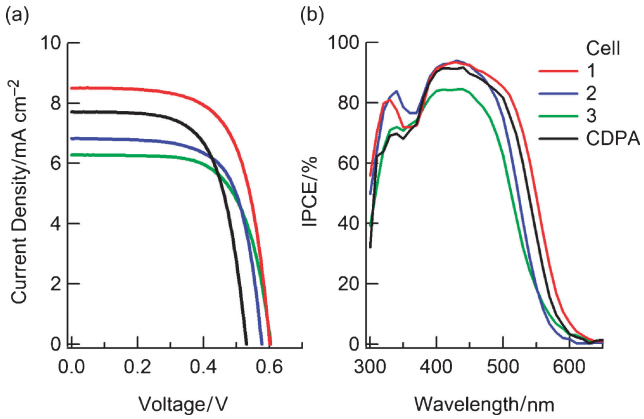

Figure 4. Photovoltaic performance for cells 1–3: (a) current density–voltage characteristics and (b) IPCE spectra.

Figure 4a shows the photocurrent density–voltage characteristics for DSCs using dyes **1**–**3** and CDPA, which are noted as cells 1–3 and cell CDPA, respectively.[14,19] The photocurrent density of cell 1 was greater than for cell CDPA over the observed voltage region, indicating a photocurrent density increase caused by the introduction of *tert*-butyl groups. The short-circuit photocurrent density (J_{sc}) and open-circuit photovoltage (V_{oc}) of cell 1 were also greater than for cell CDPA (Table 2). The solar energy-to-conversion efficiency (η) of cell 1 was measured to be 3.4%, which is 1.3 times as much as for cell CDPA (2.7%).[12] Furthermore, the photocurrent density of cell 1 was higher than that of cells 2 and 3 over the observed voltage region. The J_{sc} value depends on the amine structure, although

Table 2. Photovoltaic performance of cells 1–3[a]

Cell	J_{SC} /mA cm^{-2}	V_{OC} /V	*FF*	η /%
1	8.50	0.600	0.661	3.37
2	6.82	0.577	0.681	2.68
3	6.28	0.604	0.663	2.52
CDPA	7.70	0.530	0.654	2.67
N719	18.20	0.629	0.688	7.85

[a]Ref. 19.

the V_{oc} value is observed in a similar photovoltage range. This result may be attributed to the nonplanar structure of diphenylamine in **1** and the planar structures of carbazole and phenothiazine in **2** and **3**, respectively. The nonplanar bis(4-*tert*-butylphenyl)amine moiety is therefore a good electron-donating unit for metal-free organic dyes.

The incident photo-to-current conversion efficiency (IPCE) spectra of cells 1–3 and cell CDPA were plotted as a function of wavelength (Figure 4b). The IPCE spectra of cells 1–3 displayed profiles similar to the absorption spectra obtained for TiO_2-supported films of **1**–**3** in the 350–650 nm region.[14] The maximum IPCE values for cells 1–3 and cell CDPA reached 93, 94, 84, and 91%, respectively. These values are as high as for a DSC using N719 (cell N719) (92%). However, their IPCE spectra were blue-shifted by about 200 nm from that of cell N719, and their conversion efficiencies were much lower than for cell N719 (Table 2). Therefore, more molecular design is needed for developing high efficiency organic dyes which absorb at long wavelength. Modification of the dyes into extended π-conjugation systems is in progress.

The authors are grateful to Prof. Hiroshi Segawa and Dr. Koichi Tamaki (The University of Tokyo) for the measurements of DSC characteristics. This work was supported by a Grant-in-Aid for Scientific Research (No. 20550037) from the Ministry of Education, Culture, Sports, Science and Technology, Japan. We thank the Instrument Center of the Institute for Molecular Science for the X-ray crystallography.

References and Notes

1 a) M. Grätzel, *Inorg. Chem.* **2005**, *44*, 6841. b) A. Hagfeldt, M. Grätzel, *Chem. Rev.* **1995**, *95*, 49. c) B. O'Regan, M. Grätzel, *Nature* **1991**, *353*, 737.

2 M. K. Nazeeruddin, F. De Angelis, S. Fantacci, A. Selloni, G. Viscardi, P. Liska, S. Ito, B. Takeru, M. Grätzel, *J. Am. Chem. Soc.* **2005**, *127*, 16835.

3 a) W. Zeng, Y. Cao, Y. Bai, Y. Wang, Y. Shi, M. Zhang, F. Wang, C. Pan, P. Wang, *Chem. Mater.* **2010**, *22*, 1915. b) G. Zhang, H. Bala, Y. Cheng, D. Shi, X. Lv, Q. Yu, P. Wang, *Chem. Commun.* **2009**, 2198. c) S. Hwang, J. H. Lee, C. Park, H. Lee, C. Kim, C. Park, M.-H. Lee, W. Lee, J. Park, K. Kim, N.-G. Park, C. Kim, *Chem. Commun.* **2007**, 4887. d) D. P. Hagberg, T. Edvinsson, T. Marinado, G. Boschloo, A. Hagfeldt, L. Sun, *Chem. Commun.* **2006**, 2245.

4 a) D. P. Hagberg, J.-H. Yum, H. Lee, F. De Angelis, T. Marinado, K. M. Karlsson, R. Humphry-Baker, L. Sun, A. Hagfeldt, M. Grätzel, M. K. Nazeeruddin, *J. Am. Chem. Soc.* **2008**, *130*, 6259. b) Z. Ning, Q. Zhang, W. Wu, H. Pei, B. Liu, H. Tian, *J. Org. Chem.* **2008**, *73*, 3791.

5 a) S. Kim, J. K. Lee, S. O. Kang, J. Ko, J.-H. Yum, S. Fantacci, F. De Angelis, D. Di Censo, M. K. Nazeeruddin, M. Grätzel, *J. Am. Chem. Soc.* **2006**, *128*, 16701. b) H. Qin, S. Wenger, M. Xu, F. Gao, X. Jing, P. Wang, S. M. Zakeeruddin, M. Grätzel, *J. Am. Chem. Soc.* **2008**, *130*, 9202. c) H. Choi, C. Baik, S. O. Kang, J. Ko, M.-S. Kang, M. K. Nazeeruddin, M. Grätzel, *Angew. Chem., Int. Ed.* **2008**, *47*, 327.

6 a) N. Koumura, Z.-S. Wang, S. Mori, M. Miyashita, E. Suzuki, K. Hara, *J. Am. Chem. Soc.* **2006**, *128*, 14256. b) Z.-S. Wang, N. Koumura, Y. Cui, M. Takahashi, H. Sekiguchi, A. Mori, T. Kubo, A. Furube, K. Hara, *Chem. Mater.* **2008**, *20*, 3993.

7 C. Teng, X. Yang, C. Yuan, C. Li, R. Chen, H. Tian, S. Li, A. Hagfeldt, L. Sun, *Org. Lett.* **2009**, *11*, 5542.

8 a) Z.-S. Wang, Y. Cui, Y. Dan-oh, C. Kasada, A. Shinpo, K. Hara, *J. Phys. Chem. C* **2007**, *111*, 7224. b) K. Hara, Y. Dan-oh, C. Kasada, Y. Ohga, A. Shinpo, S. Suga, K. Sayama, H. Arakawa, *Langmuir* **2004**, *20*, 4205.

9 a) S. Ito, H. Miura, S. Uchida, M. Takata, K. Sumioka, P. Liska, P. Comte, P. Péchy, M. Grätzel, *Chem. Commun.* **2008**, 5194. b) T. Horiuchi, H. Miura, K. Sumioka, S. Uchida, *J. Am. Chem. Soc.* **2004**, *126*, 12218.

10 a) H. Tian, X. Yang, R. Chen, Y. Pan, L. Li, A. Hagfeldt, L. Sun, *Chem. Commun.* **2007**, 3741. b) H. Tian, X. Yang, J. Cong, R. Chen, J. Liu, Y. Hao, A. Hagfeldt, L. Sun, *Chem. Commun.* **2009**, 6288.

11 a) S. Eu, T. Katoh, T. Umeyama, Y. Matano, H. Imahori, *Dalton Trans.* **2008**, 5476. b) S. Mori, M. Nagata, Y. Nakahata, K. Yasuta, R. Goto, M. Kimura, M. Taya, *J. Am. Chem. Soc.* **2010**, *132*, 4054. c) H. Imahori, S. Hayashi, H. Hayashi, A. Oguro, S. Eu, T. Umeyama, Y. Matano, *J. Phys. Chem. C* **2009**, *113*, 18406.

12 a) T. Kitamura, M. Ikeda, K. Shigaki, T. Inoue, N. A. Anderson, X. Ai, T. Lian, S. Yanagida, *Chem. Mater.* **2004**, *16*, 1806. b) W. Xu, B. Peng, J. Chen, M. Liang, F. Cai, *J. Phys. Chem. C* **2008**, *112*, 874. c) D. P. Hagberg, T. Marinado, K. M. Karlsson, K. Nonomura, P. Qin, G. Boschloo, T. Brinck, A. Hagfeldt, L. Sun, *J. Org. Chem.* **2007**, *72*, 9550.

13 Z. Ning, H. Tian, *Chem. Commun.* **2009**, 5483.

14 Supporting Information is available electronically on the CSJ-Journal Web site, http://www.csj.jp/journals/chem-lett/index.html.

15 The CV measurements of **1**–**3** and CDPA were performed in acetonitrile with 0.1 M *n*-Bu_4NPF_6 at a scanning rate of 100 mV s^{-1} using Pt and Ag/Ag^+ electrodes. Potentials measured versus Fc/Fc^+ were converted to the NHE scale by addition of +0.63 V.

16 A polymorph of CDPA was reported, see: S. P. Anthony, S. Varughese, S. M. Draper, *Chem. Commun.* **2009**, 7500.

17 CCDC-767889 and -767890 contain the supplementary crystallographic data for this paper. These data can be obtained free of charge from The Cambridge Crystallographic Data Centre via www.ccdc.cam.ac.uk/data_request/cif.

18 The cocrystal was identified to have a 1:1 molar ratio of **1** and acetonitrile.

19 DSC conditions: irradiated light: AM 1.5 (100 mW cm^{-2}); photoelectrode: TiO_2 (16–19 μm thickness and 0.16 cm^2 area); electrolyte: 0.60 M 1,2-dimethyl-3-propylimidazolium iodide (DMPII)/0.025 M iodine (I_2)/0.10 M lithium iodide (LiI) in acetonitrile.

